The Steady Two-dimensional Flow of Viscous Incompressible Fluid Past an Elliptic Valve of Zero Angle of Attack Placed in a Rectilinear Channel——As a Model of a Flow Past a Fully Open Butterfly Valve

By

Akira YADA, Takeo SAKURAI and Hidenori TAKEDA

Abstract

We studied the steady two-dimensional flow of a viscous incompressibe fluid past an elliptic valve of zero angle of attack placed in a rectilinear channel. We apply generalized curvilinear coordinates, by which the channel walls and the valve surface are mapped onto corresponding coordinate lines, to the solution of the stream function-vorticity formulation of the Navier-Stokes equations. The ADI and the Euler explicit method of solution are applied to solve the transformed basic equations.

Flow patterns, pressure distributions and drag coefficients are obtained for several values of Reynolds number between 0 and 40.

Symbols

C_D = drag coefficient of the valve

J = Jacobian of the coordinate transformation

L_0 = characteristic length (half-width of the channel)

p = pressure

P, Q = functions used for an arbitrary gathering of the transformed coordinate lines

R = Reynolds number

t = time

$\underline{u}$ = velocity

u, v = x- and y- components of the velocity, respectively

U_0 = characteristic velocity (mean velocity on the upstream boundary)

x_0 = distance from the origin to the upstream and the downstream boundaries

x, y = Cartesian coordinates

x, y = x- and y- components of the force, respectively

$\alpha, \beta, \gamma =$ coordinate transformation parameters

μ $=$ viscosity

ξ, η $=$ transformed coordinates

ρ $=$ density

τ $=$ shearing stress

ψ $=$ stream function

ω $=$ vorticity

Δ $=$ Laplacian

    Non-dimensionalization of the physical variables. Original variables with dimensions are denoted by ( )*.

$x^* = L_0 x,\ y^* = L_0 y,$

$\underline{u}^* = U_0 \underline{u},$

$t^* = (L_0/U_0)\,t,$

$\rho^* = \rho_0 = \text{const},$

$p^* = \rho_0 U_0^2 R p,$

$\tau^* = \mu(U_0/L_0)\,\tau.$

1. Introduction

    Butterfly valves are widely used because of their simplicity and versatility.

    Kimura et al. (1980a, b) studied the flow past a butterfly valve in detail and determined the pressure drop due to the valve, its drag coefficient and other flow parameters from both the experimental and the theoretical view points. They also discussed the flow configuration around the valve based on an approximate method of solution. Yamashita (1980) studied Stokes flow in a channel past a flat valve with finite angle of attack and clarified the effect of angle of attack on the flow parameters.

    Although basic data necessary for the design of a butterfly valve may be obtained from the above studies, the exact solution of the flow past a valve would be of value

The Steady Two-dimensional Flow of Viscous Incompressible Fluid Past an Elliptic Valve of Zero Angle of Attack Placed in a Rectilinear Channel

39

for further improvement of the valve.

We study a steady two-dimensional flow of viscous incompressible fluid past an elliptic valve of zero angle of attack placed in a rectilinear channel. This is a model of the flow past a fully open butterfly valve.

We use a system of generalized curvilinear coordinates proposed by Thompson et al. (1976) by which the channel walls and the valve surface are mapped onto the corresponding coordinate lines. With this procedure, the numerical solution of basic equations can be performed on a rectangular field of variables. The greatest merit of this system of coordinates is that no interpolation is required in relation to boundary conditions. This method further has the merit that we can arbitrarily gather grid points to yield sufficient spatial resolution in the regions of interest.

We use the stream function-vorticity formulation of the Navier–Stokes equations. The ADI method of solution is used to solved the Poisson equation which relates the stream function and the vorticity. The Euler explicit method of solution is applied to the time integration of the momentum equation. The step size of the time integration is constrained to be within the viscous diffusion time, so that the integration may be carried out without numerical instability.

Formulation of the problem and numerical procedures are given in section 2. Results and discussion are given in section 3.

2. Basic equations in a generalized system of coordinates

The generalized system of curvilinear coordinates or 'body–fitted curvilinear coordinates' was proposed by Thompson et al. (1976), and its application is fully discussed by Themes et al. (1977) and Thompson et al. (1977). Although the basic formulas are the same as those in the above papers, we will recapitulate here in order to be self contained.

2.1 Generalized system of curvilinear coordinates

Let us suppose a steady two-dimensional flow of viscous incompressible fluid past an elliptic valve of zero angle of attack placed in a rectilinear channel. The ratio of axes of the ellipse is set equal to 0.2. The upstream and the downstream boundaries, on which the in-flow and the out-flow conditions are imposed, are located at $x = -20$. and $x = +20$., respectively.

Following the basic idea of body–fitted curvilinear coordinates proposed by Thompson et al. (1976), we transform the physical plane of the above geometry onto a rectangular computational plane. Figs. 1 and 2 illustrate two kinds of mapping procedures. Fig. 1 shows an 'O-type' transformation, in which the grid points in the physical plane are aligned along O-shaped curves and are attracted to the valve surface.
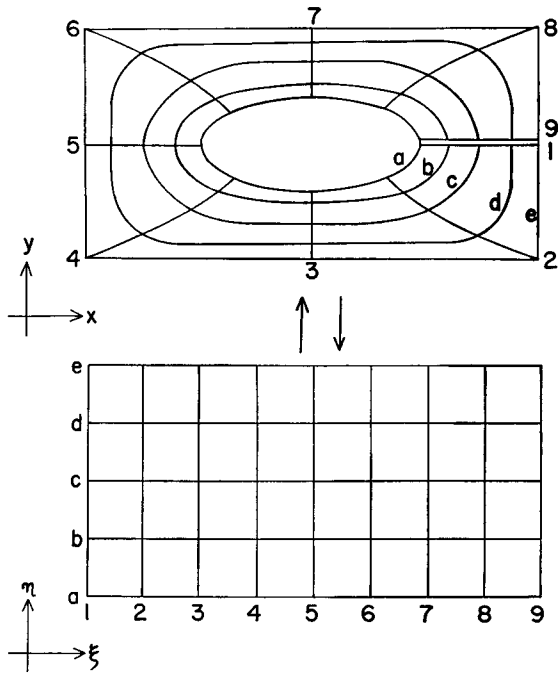
Fig. 1. Correspondence between the physical plane and the calculation plane for the case of an O-type grid. Corresponding lines have the same symbols.
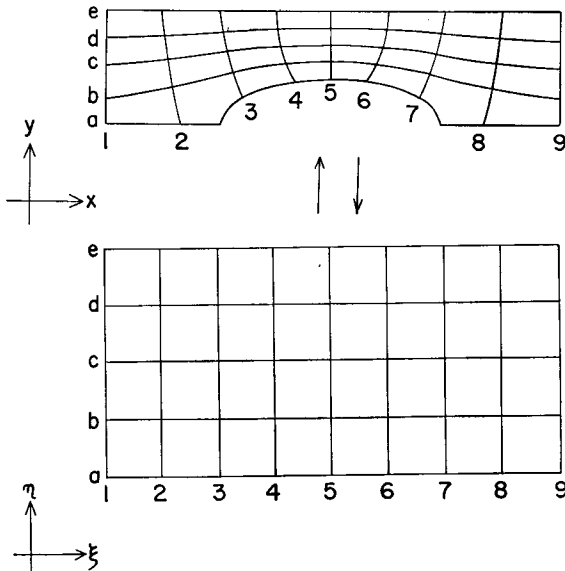

Fig. 2. Correspondence between the physical plane and the calculation plane for the case of an H-type grid. Corresponding lines have the same symbols.

This type of transformation is convenient for detailed study of the flow pattern in the immediate neighbourhood of the valve. Fig. 3 shows an example of the 81×60 generated coordinate lines. Fig. 2 illustrates an 'H-type' transformation in which grid points in the physical plane are aligned along approximate stream lines. This type of transformation is convenient for studying the pressure distribution along channel walls and thus the pressure drop caused by the valve. Fig. 4 shows an example of the 121×20 generated coordinate lines.

The mapping functions;

$$x = x(\xi, \eta),\qquad (2\text{-}1)$$

$$y = y(\xi, \eta),\qquad (2\text{-}2)$$

satisfy Poisson type equations on the mapped plane:

$$\alpha x_{\xi\xi} - 2\beta x_{\xi\eta} + \gamma x_{\eta\eta}$$
$$= -J^2[x_\xi P(\xi, \eta)$$
$$+ x_\eta Q(\xi, \eta)],\quad (2\text{-}3)$$
$$\alpha y_{\xi\xi} - 2\beta y_{\xi\eta} + \gamma y_{\eta\eta}$$
$$= -J^2[y_\xi P(\xi, \eta)$$
$$+ y_\eta Q(\xi, \eta)],\quad (2\text{-}4)$$

where

$$\alpha = x_\eta^2 + y_\eta^2,\qquad (2\text{-}5)$$

$$\beta = x_\xi x_\eta + y_\xi y_\eta,\qquad (2\text{-}6)$$

$$\gamma = x_\xi^2 + y_\xi^2,\qquad (2\text{-}7)$$

$$J = x_\xi y_\eta - x_\eta y_\xi.\qquad (2\text{-}8)$$

This system is a quasi-linear elliptic system for the coordinate functions $x(\xi, \eta)$ and $y(\xi, \eta)$ in

The Steady Two-dimensional Flow of Viscous Incompressible Fluid Past an Elliptic Valve of Zero Angle of Attack Placed in a Rectilinear Channel

41

the transformed plane. Solution of the elliptic system assures us that the Jacobian of the transformation does not vanish except at isolated singular points. Boundary conditions are specified on straight boundaries, and the spacing of the coordinate lines in the transformed plane is uniform. The inhomogeneous terms $P(\xi, \eta)$ and $Q(\xi, \eta)$ are sums of decaying exponential functions which allow us to attract coordinate lines towards specified lines and points in the physical plane.
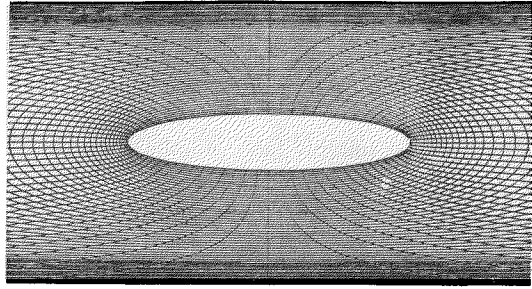

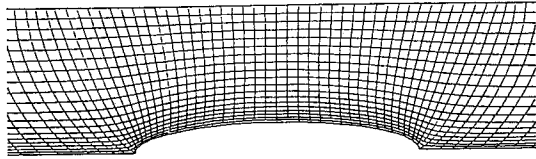Fig. 3. An example of generated coordinate lines for the case of an O-type grid.

Fig. 4. An example of generated coordinate lines for the case of an H-type grid.

2.2 Basic equations in the transformed plane

The stream function–vorticity formulation of the Navier-Stokes equations of the two-dimensional flow of viscous incompressible fluid is given as follows:

$$\omega_t + \phi_y\omega_x - \phi_x\omega_y = (\omega_{xx} + \omega_{yy})/R, \tag{2-9}$$

$$\phi_{xx} + \phi_{yy} = -\omega, \tag{2-10}$$

where ϕ is the non-dimensional stream function, ω the non-dmensional vorticity, and R the Reynolds number based on the mean velocity on the upstream boundary and the half-width of the channel.

The transformation discussed in 2.1 transforms equations (2-9) and (2-10) as follows:

$$\omega_t + (\phi_\eta\omega_\xi - \phi_\xi\omega_\eta)/J = (\alpha\omega_{\xi\xi} - 2\beta\omega_{\xi\eta} + \gamma\omega_{\eta\eta})/J^2R + (Q\omega_\eta + P\omega_\xi)/R, \tag{2-11}$$

$$(\alpha\phi_{\xi\xi} - 2\beta\phi_{\xi\eta} + \gamma\phi_{\eta\eta})/J^2 + Q\phi_\eta + P\phi_\xi = -\omega. \tag{2-12}$$

For the case where the Reynolds number is equal to zero, (2-9) and (2-11) are respectively modified as follows:

$$\omega_t = \omega_{xx} + \omega_{yy}, \tag{2-13}$$

$$\omega_t = (\alpha\omega_{\xi\xi} - 2\beta\omega_{\xi\eta} + \gamma\omega_{\eta\eta})/J^2 + Q\omega_\eta + P\omega_\xi. \tag{2-14}$$

2.3 Boundary conditions

Boundary conditions for the stream function ϕ are of Dirichlet type, corresponding to the situation in which the velocity distribution becomes of Poiseuille type at the

upstream and the downstream boundaries, the in-flow and the out-flow conditions on ϕ are given by

$$\phi = (y - y^3/3) \cdot (3/2) \quad \text{at } x = \pm x_0, \tag{2-15}$$

where x_0 is a suitably large number to ensure sufficient accuracy. On the upper and the lower wall of the channel, ϕ is $+1.0$ and -1.0, respectively. On the stagnation stream line, ϕ is zero.

On the upstream and the downstream boundaries, that is $x = \pm x_0$, the spatial derivative of ω with respect to the stream-wise direction is set equal to zero (Roache 1972a),

i.e. $\quad \partial \omega / \partial x = 0. \tag{2-16}$

Based on the no-slip condition and equation (2-12), ω on the rigid wall boundaries is set as follows (Roache 1972b):

$$\omega = -\gamma \phi_{\eta\eta}/J^2 \quad \text{on } y = +1 \text{ and } -1 \text{ and on the valve surface,} \tag{2-17}$$

where the right hand side is to be calculated on the respective boundaries.

2.4 Numerical procedure

Equation (2-12) is solved by the ADI method of solution. The criterion of the convergence is that the absolute relative increment of the stream function with respect to the iteration is less than a certain tolerance ε;

$$|(\phi^{k+1} - \phi^k)/\phi^{k+1}| < \varepsilon, \tag{2-18}$$

where k refers to the iteration step. To avoid unnecessarily strict application of the criterion near the zero stream line, this criterion is applied to the flow region for which

$$|\phi^{k+1}| > \delta, \tag{2-19}$$

where δ is a certain infinitesimal. In our calculation, ε and δ are set to be 10^{-2} and 10^{-4}, respectively.

Time integration of equation (2-11) (or (2-14)) is carried out by the Euler explicit method. The step size is equal to the viscous diffusion time multiplied by a factor. The factor is taken rather small ($\sim 10^{-3}$) at the beginning and is increased gradually to reach the final value of 0.5.

These procedures are successively carried out until the relative time derivative of the vorticity becomes less than a certain tolerance. The criterion is given as:

$$|\omega_t|/[|\phi_\eta \omega_\xi/J| + |\phi_\xi \omega_\eta/J| + (|\alpha \omega_{\xi\xi}| + |2\beta \omega_{\xi\eta}| + |\gamma \omega_{\eta\eta}|)/J^2 R$$
$$+ (|Q\omega_\eta| + |P\omega_\xi|)/R] < \varepsilon', \tag{2-20}$$

The Steady Two-dimensional Flow of Viscous Incompressible Fluid Past an Elliptic Valve of Zero Angle of Attack Placed in a Rectilinear Channel

43

for the case of non-vanishing Reynolds number and as:

$$|\omega_t|/[(|\alpha\omega_{\xi\xi}|+|2\beta\omega_{\xi\eta}|+|\gamma\omega_{\eta\eta}|)/J^2+|Q\omega_\eta|+|P\omega_\xi|]<\varepsilon', \qquad (2\text{-}21)$$

for the case of vanishing Reynolds number.

Based on the same reasoning as in (2-19), (2-20) or (2-21) is applied to the flow region for which,

$$|\omega|>\delta'|\omega|_{MAX}, \qquad (2\text{-}22)$$

where ε' and δ' are infinitesimals as above. (Typically $\varepsilon'=10^{-2}$, $\delta'=0.2$)

2.5 Pressure coefficient

Once the velocity distribution is determined, the pressure is obtained by a line integral based on the primitive form of the Navier-Stokes equations. We start our integration from the upstream boundary and set the starting value of the pressure to be zero.

The integration is performed along channel walls and along the stagnation stream line. Based on the correspondence between the (x, y)-plane and the (ξ, η)-plane in the case of the O-type grid, we can take the integrals along the channel wall and along the valve surface as the integrals with respect to ξ for respectively fixed values of η:

$$
\begin{aligned}
P(\xi_0)-P(\xi) &=\int_\xi^{\xi_0}dP=\int_\xi^{\xi_0}(\partial p/\partial\xi)\,d\xi \\
&=\int_\xi^{\xi_0}[-R((u^2/2)_x-\omega v)x_\xi+\varDelta u x_\xi-R((u^2/2)_y+\omega u)y_\xi+\varDelta v y_\xi]d\xi \\
&=-R[u^2/2]_\xi^{\xi_0}+\int_\xi^{\xi_0}[-R\omega\psi_\xi+(\beta\omega_\xi-\gamma\omega_\eta)/J]d\xi. \qquad (2\text{-}23)
\end{aligned}
$$

Because the flow is symmetric with respect to y in our case of zero angle of attack, integrals along the upstream-branch and the downstream-branch of the stagnation stream line can be taken as those with respect to η for respectively fixed value of ξ:

$$P(\eta_0)-P(\eta)=-R[u^2/2]_\eta^{\eta_0}+\int_\eta^{\eta_0}[-R\omega\psi_\eta+(\alpha\omega_\xi-\beta\omega_\eta)/J]d\eta. \qquad (2\text{-}24)$$

If we use the H-type grid, the integrals are all with respect to ξ for respectively fixed values of η. This situation can easily be seen based on the correspondence between the (x, y)-plane and the (ξ, η)-plane (see Fig. 2).

2.6 Drag coefficient

The force on the valve surface is given as

$$x = [-p + 2(\partial u/\partial x)](-y_\xi) + [(\partial u/\partial y) + (\partial v/\partial x)]x_\xi, \qquad (2\text{-}25)$$

$$Y = [(\partial u/\partial y) + (\partial v/\partial x)](-y_\xi) + [-p + 2(\partial v/\partial y)]x_\xi, \qquad (2\text{-}26)$$

where X and Y is the x- and y-component of the force respectively, and use is made of the fact that η is constant on the surface.

Combining the equation of continuity and the no-slip conditions on the valve surface, we obtain:

$$-(\partial v/\partial y)x_\xi + (\partial u/\partial y)y_\xi = 0, \qquad (2\text{-}27)$$

$$(\partial v/\partial x)x_\xi - (\partial u/\partial x)y_\xi = 0. \qquad (2\text{-}28)$$

Using the above, X and Y are modified as follows:

$$\begin{aligned} X &= py_\xi + [-(\partial v/\partial x) + (\partial u/\partial y)]x_\xi \\ &= py_\xi - \omega x_\xi, \end{aligned} \qquad (2\text{-}29)$$

$$\begin{aligned} Y &= -px_\xi + [-(\partial v/\partial x) + (\partial u/\partial y)]y_\xi \\ &= -px_\xi - y_\xi. \end{aligned} \qquad (2\text{-}30)$$

Drag coefficient C_D is obtained by the integration of X along the valve surface:

$$C_D = (1/R)\int_{\xi_{min}}^{\xi_{max}} (py_\xi - \omega x_\xi)\,d\xi, \qquad (2\text{-}31)$$

where the factor $(1/R)$ is inserted because of our definition of the non-dimensional drag force.

The lift coefficient i.e. the corresponding integral of Y vanishes because of the symmetry of our flow.

3. Discussion

3.1 The results

We studied cases with Reynolds numbers $0, 3, 7, 10, 20, 30$ and 40. These may seem to be rather small from a practical view point, but Imai (1958) has pointed out that if we restrict our attention to the time average, we can get a reasonable model of a high Reynolds number flow about a bluff body from a steady flow with an effective Reynolds number of 40.

To examine the accuracy of our solution in relation to the finite value of x_0, we compare a flow of Reynolds number 40 for $x_0 = 20$ (Figs. 5-1 to 5-4) with that for $x_0 = 15$ (Figs. 7-1 to 7-4). Both flow patterns show good agreement near the valve and the drag coefficient C_D agree to within the order of 1%. Based on these results, we use the value of $x_0 = 20$ for all the other solutions.

A merit of the O-type grid is that the no-slip condition on the valve surface is satisfied to a good accuracy. For example, the largest value of the slipping velocity was

0. 0156 for the case with Reynolds number of 40. The reason is that there are a sufficient number of lines of constant η around the valve to give good resolution. As the demerit of this grid system, the pressure distribution on the channell wall could not be calculated with reasonable accuracy. This is because there exist only 20 grid points along the wall. Final estimates of the relative error of ω_t are given in Figs. 5-4, 6-4 and 7-4. *H*-type grid, in contrast, has 121 grid points both on the stagnation stream line and on the channell wall, and the pressure distribution is calculated to a high accuracy on both lines. Because grid spacing near the valve is rather sparse in comparison with that in the *O*-type grid, however, the no-slip condition on the valve is rather poorly satisfied. The largest value of the slipping velocity is 0. 1223 for the flow with Reynolds number 40. The relative errors of ω_t are below 0. 01 in the vicinity of the valve, and at most 0. 06 in the entire field. The relative error in this case, therefore, is not presented. These assure us that the final step of our calculation can be taken as the steady limit of the unsteady flow.

The flow patterns of the steady limit for various Reynolds numbers are given in Figs. 5-1 to 8-3.
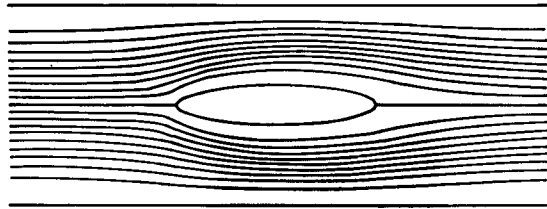
Fig. 5-1. Stream lines for a case with $R=40$ and $x_0=20$. The *O*-type grid is used.
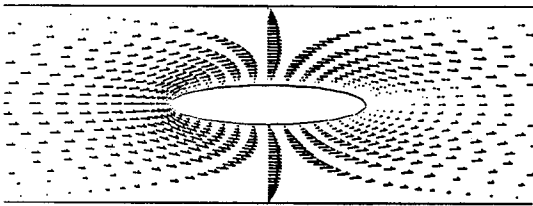
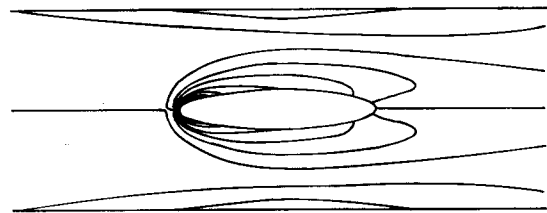Fig. 5-2. Velocity vectors for a case with $R=40$ and $x_0=20$. The *O*-type grid is used.

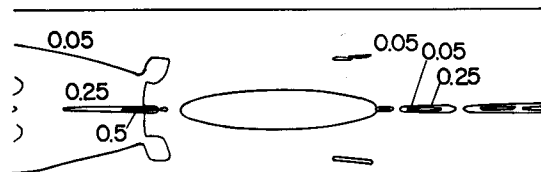Fig. 5-3. Equi-vorticity lines for a case with $R=40$ and $x_0=20$. The *O*-type grid is used.

Fig. 5-4. A contour representation of the steadiness parameter r for a case with $R=40$ and $x_0=20$, where
$$r=|\omega_t|/[(|\psi_\eta\omega_\xi/J|+|\psi_\xi\omega_\eta/J| +(|\alpha\omega_{\xi\xi}|+|2\beta\omega_{\xi\eta}|+|\gamma\omega_{\eta\eta}|)/J^2R +(|Q\omega_\eta|+|P\omega_\xi|)/R]$$
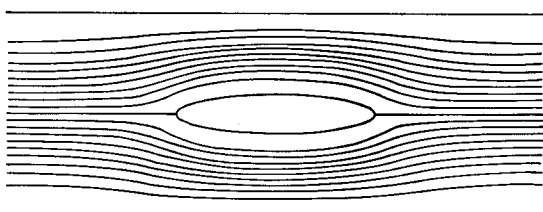The numbering of each contour gives the value of r. The *O*-type grid is used.

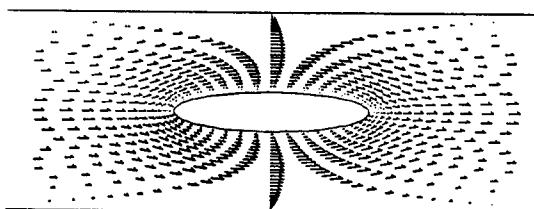Fig. 6-1.   Stream lines for a case with $R=0$. The O-type grid is used.

Fig. 6-2.   Velocity vectors for a case with $R=0$. The O-type grid is used.
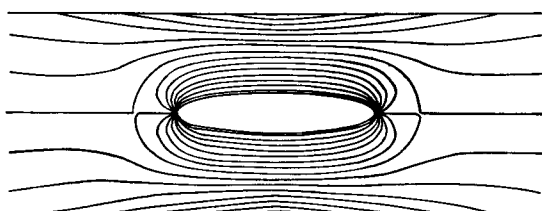

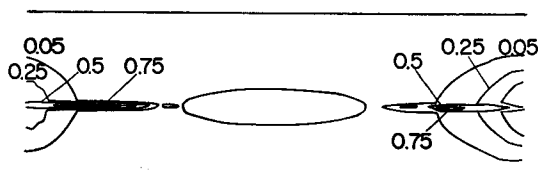Fig. 6-3.   Equi-vorticity lines for a case with $R=0$. The O-type grid is used.

Fig. 6-4.   A contour representation of the steadiness parameter r for a case with $R=0$, where
$$r=|\omega_t|/[(|\alpha\omega_{\xi\xi}|+|2\beta\omega_{\xi\eta}| +|\gamma\omega_{\eta\eta}|)/J^2+|Q\omega_\eta|+|P\omega_\xi|].$$
The numbering of each contour gives the value of r. The O-type grid is used.

Figs. 6-1 to 6-3 clarify that the flow pattern for the case of $R=0$ is symmetric with respect to x. Figs. 5-1 to 5-3 clarify, on the contrary, that the flow pattern for the case of $R=40$ is asymmetric with respect to x. Especially, Fig. 5-3 clarifies the appearance of a region of strong vorticity near the nose. The figure also shows the existence of a region of weak vorticity near the tail. This can be taken as a sign of the flow separation for cases of higher Reynolds numbers.

Figs. 9 to 11 give the pressure distributions on the zero stream line for the O-type grid. Similar to the viscous flow of infinite extent past a sphere (cf. Landau and Lifshitz, 1959), there exist regions near the nose and tail of the valve, for which the pressure gradient $(\partial p/\partial x)$ is positive. This fact is also seen in Fig. 12-1 for the H-type grid. Comparison of Fig. 9 with Fig. 12-1 shows the superiority of the H-type grid over the O-type grid as far as the pressure distribution outside the valve is concerned. The comparison also shows that the pressure distributions on the valve surface agree well with each other. The pressure distribution on a channel wall is given in Fig. 12-2. The pressure distribution on a channel wall agrees well with that on the zero stream line except near the

valve. There exists a region of positive pressure gradient also on the channel wall.

The largest discrepancy between the drag coefficient using the O-type grid and the H-type grid is 2.54% for the flow with Reynolds number 40. The drag coefficient versus Reynolds number is given in Fig. 13. For the sake of compactness of the figure, we use RC_D rather than C_D as the ordinate. Based on results for Reynolds number 20 and 40, we can determine coefficients of Imai's formula (1958) of the drag coefficient:

$$C_D{}^{1/2} = 0.212 + 6.90 R^{-1/2}$$
$$(3-1)$$

We can also get a simple linear relation between C_D and R^{-1}:

$$C_D = 0.308 + 55.5/R.$$
$$(3-2)$$

The estimate of RC_D by (3-1) is given by a dashed line and that by (3-2) is given by a dash-dotted line in Fig. 13. Present results agree better with (3-2) than with (3-1). This result poses an interesting problem of the channel wall correction of Imai's formula.

3.2 Concluding remarks

In the present study, we restricted our attention to cases of zero angle of attack. The method of generalised coordinate system, however, can be applied to cases
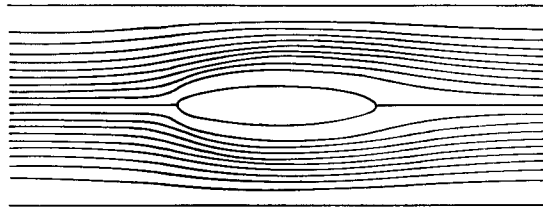

Fig. 7-1. Stream lines for a case with $R=40$ and $x_0=15$. The O-type grid is used.
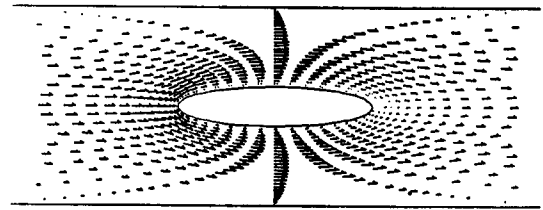

Fig. 7-2. Velocity vectors for a case with $R=40$ and $x_0=15$. The O-type grid is used.
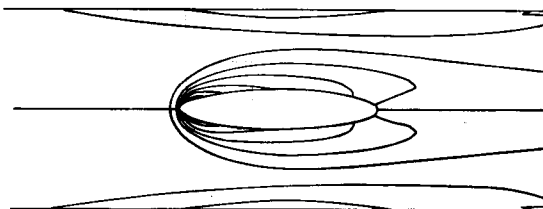

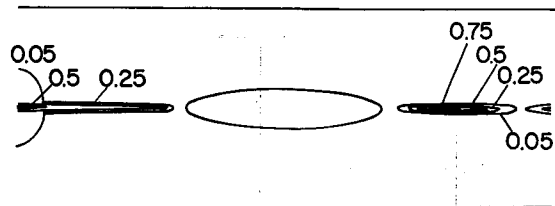Fig. 7-3. Equi-vorticity lines for a case with $R=40$ and $x_0=15$. The O-type grid is used.

Fig. 7-4. A contour representation of the steadiness parameter r for a case with $R=40$ and $x_0=15$, where
$$r = |\omega_t|/[|\psi_\eta\omega_\xi/J| + |\psi_\xi\omega_\eta/J| + (|\alpha\omega_{\xi\xi}| + |2\beta\omega_{\xi\eta}| + |\gamma\omega_{\eta\eta}|)/J^2R + (|Q\omega_\eta| + |P\omega_\xi|)/R].$$
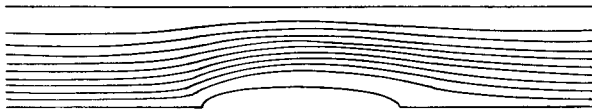The numbering of each contour gives the value of r. The O-type grid is used.

Fig. 8-1. Stream lines for a case wth $R=40$. The H-type grid is used.

Fig. 8-2. Velocity vectors for a case with $R=40$. The H-type grid is used.
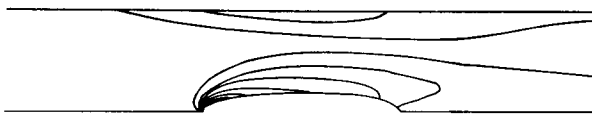

Fig. 8-3. Equi-vorticity lines for a case wth $R=40$. The H-type grid is used.
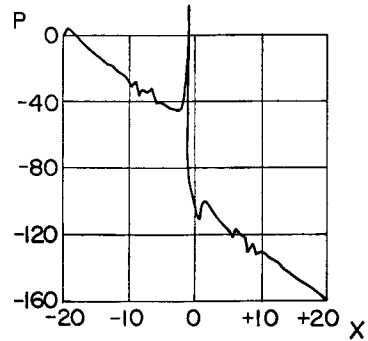

Fig. 9. The pressure distribution along the stagnation stream line for a case with $R=40$ and $x_0=20$. The O-type grid is used.
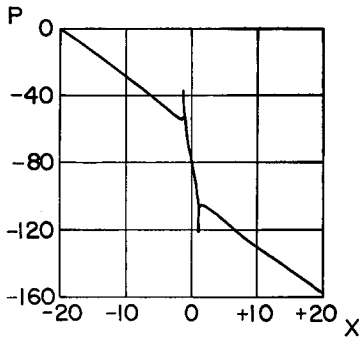

Fig. 10. The pressure distribution along the stagnation stream line for a case with $R=0$. The O-type grid is used.
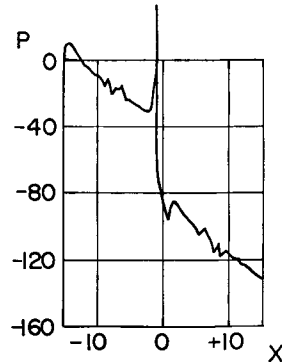

Fig. 11. The pressure distribution along the stagnation stream line for a case with $R=40$ and $x_0=15$. The O-type grid is used.
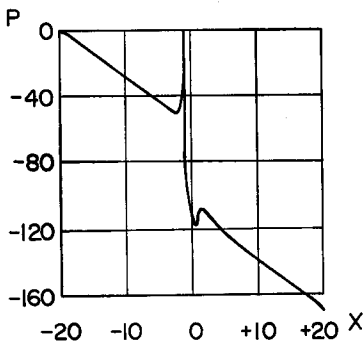

Fig. 12-1. The pressure distribution along the stagnation stream line for a case with $R=40$. The H-type grid is used.
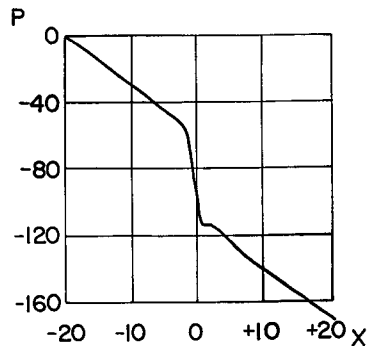

Fig. 12-2. The pressure distribution on a channel wall for a case with $R=40$. The H-type grid is used.
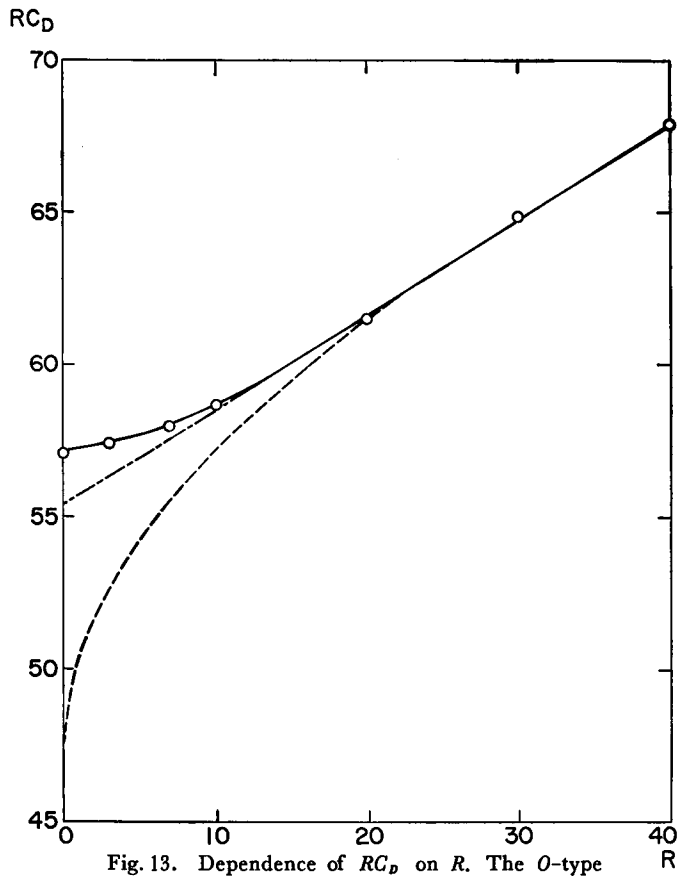
The Steady Two-dimensional Flow of Viscous Incompressible Fluid Past an
Elliptic Valve of Zero Angle of Attack Placed in a Rectilinear Channel

49

RC_D

Fig. 13. Dependence of RC_D on R. The O-type
grid is used.

with finite angle of attack. The solution can be obtained similarly to the case of zero angle of attack. An additional complication comes from the fact that the stagnation stream line is not given ab initio and is to be determined during the process of solution. As Thompson et al. (1976), Uchida (1980) and Alam et al. (1983) showed, the single-valuedness of the pressure on the valve surface can be included iteratively in the solution. This would be the easiest extension of our present study.

We thank Professor Takuya Matsuda and Doctor Izumi Hachisu for their discussions. We also thank Doctor Anthony J. Allen for kindly inspecting the manuscript.

The computations were performed on a Fujitsu *M*-382 at the Date Processing Center of Kyoto University.

References

Alam Md. S., Kawamura T., Kuwahara K., and Takami H., 1983, "Numerical Computation of the
Interaction between Bluff Bodies in a Viscous Flow", Proceedings of Institute of Mathematical

Analysis 476, Kyoto University Institute of Mathemaical Analysis, 125-143

Imai I., 1958, „Theory of Drag Force by Fluid", (in Japanese), Kagaku, vol. 28, 110-115

Kimura T., Kuwahara C., and Yoneda J., 1980a, "Study on Butterfly Valve, Characteristics of Flow Coefficient C_v", (in Japanese), KR-FO1, Faculty of Engineering, Kobe University

Kimura T., Kuwahara C., and Yoneda J., 1980b, "Study on Butterfly Valve, Characteristics of Flow, Torque, and Cavitation", (in Japanese), KR-FO2, Faculty of Engineering, Kobe University

L. D. Landau and E. M. Lifshitz, 1959, "Fluid Mechanics", Pergamon Press, Oxford, 63-66

P. J. Roache, 1972a, "Computational Fluid Dynamics", Hermosa Publishers, Albuquerque, New Mexico, 155

P. J. Roache, 1972b, "Computational Fluid Dynamics", Hermosa Publishers, Albuquerque, New Mexico, 141

Themes, F. C., Thompson, J. F., Mastin, C. W., and Walker, R. L., 1977, "Numerical Solutions for Viscous and Potential Flow about Arbitrary Two-dimensional Bodies Using Body-Fitted Coordinate System", Journal of Computational Physics, vol. 24, 245-273

Thompson, J, F., Themes, F. C., and Mastin, C. W., 1976, "Boundary-Fitted Curvilinear Coordinate System for Solution of Partial Differential Equations on Fields Containing Any Number of Arbitrary Two-dimensional Bodies", NASA CR-2729

Thompson, J. F., Themes, F. C., and Mastin, C. W., 1977, "TOMCAT -A Code for Numerical Generation of Body-Fitted Curvilinear Coordinate System on Fields Containing Any Number of Arbitrary Two-dimensional Bodies", Journal of Computational Physics, vol. 24, 274-302

Uchida H., 1980, "Analysis of Two-dimensional Viscous Flow by Finite Element Method (Applications to Engineering Problems)", (in Japanese) Proceedings of Symposium on Space Flight Dynamics, University of Tokyo, Institute of Space and Aeronautical Science, 130-136

Yamashita T., 1980, "Low Reynolds Number Flow Past a Flat Plate with Angle of Attack Placed in Two-dimensional Channel", (in Japanese), Master Thesis, Faculty of Engineering, Kyoto University